

# Robot Sound Interpretation: Learning Visual-Audio Representations for Voice-Controlled Robots

Peixin Chang, Shuijing Liu, and Katherine Driggs-Campbell

**Abstract**—Inspired by sensorimotor theory, we propose a novel pipeline for voice-controlled robots. Previous work relies on explicit labels of sounds and images as well as extrinsic reward functions. Not only do such approaches have little resemblance to human sensorimotor development, but also require hand-tuning rewards and extensive human labor. To address these problems, we learn a representation that associates images and sound commands with minimal supervision. Using this representation, we generate an intrinsic reward function to learn robotic tasks with reinforcement learning. We demonstrate our approach on three robot platforms, a TurtleBot3, a Kuka-IIWA arm, and a Kinova Gen3 robot, which hear a command word, identify the associated target object, and perform precise control to approach the target. We show that our method outperforms previous work across various sound types and robotic tasks empirically. We successfully deploy the policy learned in simulator to a real-world Kinova Gen3.

## I. INTRODUCTION

As robots begin to enter people’s daily lives, there is an increasing need for mechanisms that allow non-experts to interact and communicate with robots in an intuitive way. Spoken language is a natural choice for communication, leading to a wealth of research in voice-controlled robots [1]. Building on recent advancements in representation learning, we propose a novel pipeline for voice-controlled robots that utilizes a representation for images and sounds.

Conventional pipelines for voice-controlled robots consist of independent modules for automatic speech recognition (ASR), natural language understanding (NLU), symbol grounding, and motion planning. These pipelines suffer from intermediate and cascading errors between different modules and the difficulties in relating language to the physical entities it refers to [1]–[3]. To address these problems, end-to-end spoken language understanding (SLU) systems and end-to-end natural language grounding agents attempt to combine some of the independent modules [3], [4]. However, end-to-end SLU does not consider robotic tasks and language grounding agents use text as inputs rather than sound. Thus, neither the end-to-end SLU nor the natural language grounding agents can solve voice-controlled robot tasks alone.

The first end-to-end model for voice-controlled robots and the concept of Robot Sound Interpretation (RSI) is proposed in [5]. RSI is motivated by embodied language acquisition [6], [7] and studies how an embodied agent learns and builds its own interpretation of sounds [5]. Combining the ideas from end-to-end SLU and natural language grounding

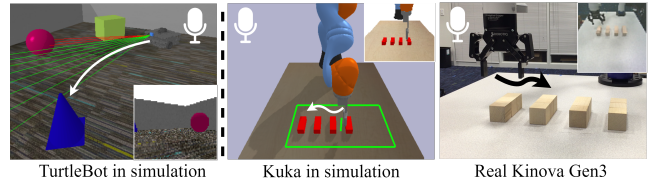


Fig. 1: **Illustration of our robotic tasks.** The robots must approach a target mentioned by a sound command. Windowed image shows the robot camera view. *Left:* The TurtleBot searches for then navigates to the target object among four objects. The green and red vectors illustrate what the robot sees but will not be used by the robot. *Middle:* The Kuka moves its gripper tip to the target block among four identical blocks. The rectangle shows the reachable region of the gripper tip and the vertical line indicates the location of the gripper tip on the table top. The robot cannot see them. *Right:* The deployment of a learned policy to a physical Kinova Gen3.

agents, the model directly maps sound commands to robot motions. However, the model has its own weaknesses such as extensively-tuned reward functions. In this paper, we address some of the problems in [5] and propose a new method for training RSI agents.

We believe that every sound conveys meaning and can be used as a command to trigger robot actions. We study the same tasks for voice-controlled robots as in [5], which is illustrated in Fig. 1. After hearing a sound command, the robot must identify and approach the corresponding target from the set of nearby objects. To achieve this goal, the robots must learn the meaning of the sound command, draw the correspondence between the visual and audio inputs, and develop a policy to search and reach the target using limited sensors. To successfully solve these tasks, a method needs to be general in terms of types of sounds, robots, and tasks.

Our method is inspired by sensorimotor contingency which is the relations between actions and the resulting sensory changes [8], [9]. Imagine that an infant takes random actions while exploring nearby objects. She touches a bell by accident and hears a bell ring. Motivated by her “intrinsic curiosity,” she attempts to replicate the sound by repeating and refining the touching action [10]. When she hears a bell ring later, she should identify what actions are needed to ring the bell. Similarly, infants can learn to associate an object with its name when they touch the object and their parents say the name of the object immediately afterwards. We believe that a robot can associate the motor actions with the corresponding sound through a similar learning process. Once the robot has developed sensorimotor contingencies from its previous embodied experiences, we can use a sound command to ask the robot to reach the goal. The ability to ground or relate language to the physical entities of the world allows the robot to communicate with humans on a

mutual understanding, which leads to much more meaningful human-robot interactions [11], [12].

Our training pipeline consists of two stages, which closely mimics the sensorimotor learning process. In the first stage, the agent collects auditory and visual observations by randomly exploring the environment. Using the collected data, we train a visual-audio representation (VAR) which maps the visual and audio inputs to vector embeddings. In the second stage, we use the VAR to produce an intrinsic reward, which is used to train the agent to reach the target and replicate a sound using reinforcement learning (RL). For example, reaching the bell produces a ringing sound. After the training, the robot will master sensorimotor contingencies and can complete tasks given a sound command.

The main contributions of this paper are: (1) We present a novel pipeline for voice-controlled robots and robot language acquisition inspired by sensorimotor theory. (2) We build a novel representation for images and sounds, which is used as intrinsic reward function for RL. (3) Our network exhibits promising results in three robot platforms: a Kuka-IIWA, a TurtleBot3, and a Kinova Gen3. The Kinova Gen3 policy was successfully transferred to a real-world Kinova Gen3 without training on real-world data.

This paper is organized as follows: we review related works in Section II. In Section III, we introduce our pipeline. We discuss simulated and real-world experiments in Section IV and Section V, respectively. Finally, we conclude the paper in Section VI.

## II. RELATED WORKS

### A. Conventional voice-controlled robots

The usual pipeline of conventional voice-controlled robots consists of an ASR system to transcribe speech to text [13], an NLU system to map text transcripts to speaker intent [2], [14], a grounding module to associate the intent with physical entities [15], [16], and a planner to generate feasible trajectories for robot task execution [1], [17]–[19]. However, the pipeline suffers from several limitations. First, off-the-shelf ASR systems usually operate in a general-purpose setting irrelevant to specific robotic tasks and their outputs could be inevitably out-of-context or erroneous [2], [20], [21]. Typical NLU systems, however, are trained on clean text [4]. Thus, the overall robotic task performance degrades due to the intermediate errors. Second, even if the NLU produces the correct speaker intention, the robots may still have difficulties in connecting words with what they perceive because this grounding process requires complex reasoning and perceptual skills such as detection, recognition, and estimation. Rule-based systems and methods based on symbolic AI have been used for grounding [22], [23]. However, developing such system requires significant labor and does not scale beyond their programmed domains [2], [3].

### B. End-to-end language understanding and grounding

Different from the conventional ASR plus NLU pipeline, the end-to-end SLU system maps the speech directly to the speaker’s intent without translating the speech to text [4],

[24]–[27]. The end-to-end learning avoids the intermediate errors and allows the models to fully exploit subtle information such as speaker emotion, music, and background noise that will be lost during transcription [24], [26]. Besides, the end-to-end SLU system mimics how humans extract intent-level concepts. Instead of understanding the speech by recognizing word by word, humans directly interpret high-level concepts in speech [4]. However, end-to-end SLU systems are mainly used for virtual digital assistants and do not consider the complex grounding process in robotics.

End-to-end language grounding agents have been developed to perform tasks such as navigation [28]–[30] and object finding [3], [31] according to text-based natural language instructions and visual observations. Our work is different from them in several aspects. First, we focus on voice-controlled agents, while the above works consider text-based input which limit the potential of human-robot communication. Second, training these agents require either human-annotated ground-truth trajectories for imitation learning [28], [29] or a carefully designed extrinsic reward function for reinforcement learning [3], [30], [31]. In contrast, our method needs neither the human demonstrations nor extrinsic reward functions.

### C. Robot Sound Interpretation

The first method that combines the ideas from end-to-end SLU and language grounding agents for voice-controlled robots is proposed in [5]. An end-to-end deep learning model directly maps sound commands and visual signals to a sequence of robot actions that fulfill the commands. The model is trained using RL with auxiliary losses for image and sound feature extraction. However, the method has several problems. First, the language grounding and skill learning are highly coupled because of the end-to-end training. Thus, the trained model or representation cannot be reused for other tasks. Second, carefully designed extrinsic reward functions are necessary for the success of reinforcement learning. Third, the sound commands are separated from the robotic environment, but children develop their language skills in interactive environments [32], [33]. Finally, the RL training heavily depends on the explicit one-hot labels of sound commands and images for the auxiliary losses. The one-hot labels not only require extensive human labor to obtain but also leads to an extremely large classification layer in the network as the vocabulary of the sound commands increases.

To address these problems, our pipeline separates the language grounding and skill learning modules. Our method requires neither an extrinsic reward nor explicit labels to train an RSI agent. Our new environment gives audio feedback to help the agent learn the meanings of sounds.

### D. Representation learning for robotics

Representation learning has shown great potential in learning useful embeddings for downstream control tasks. Deep autoencoders are used to encode high-dimensional observations such as images into lower-dimensional embeddings. These vectors are then used as states or intrinsic reward

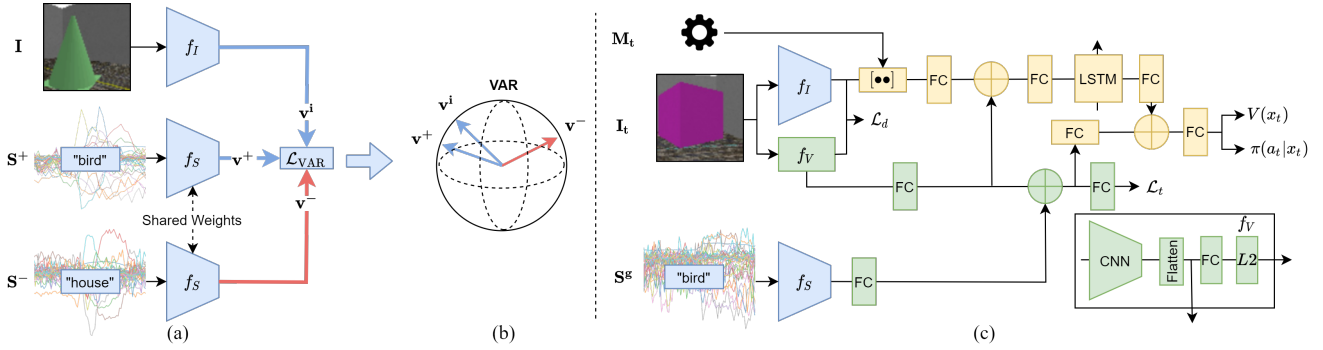


Fig. 2: **The network architectures.** (a) The VAR is a three-branch Siamese network optimized with triplet loss. (b) The latent space of the VAR is a unit hypersphere such that vector embeddings of images and audios of the same object are closer than those of different objects. (c) The policy network for RL training. The loss  $\mathcal{L}_d$  and  $\mathcal{L}_t$  are only needed to solve the TurtleBot environment. The portion to be pretrained is in green. The portion in blue is VAR and the weights are frozen in RL training. We use  $\oplus$  to denote element-wise addition,  $FC$  to denote fully connected layers, and  $[\bullet\bullet]$  to denote concatenation.

functions for reinforcement learning [34]–[36]. At test time, however, the methods in [35], [36] require users to provide goal images for task execution, which is an unnatural and inconvenient way of human-robot communication compared to voice control. On the other hand, contrastive loss is used to learn representations for downstream tasks such as grasping and water pouring [37]–[39]. One advantage of using contrastive loss is that the loss avoids the reconstruction required by autoencoders. However, these works focus mainly on the visual or the text modality and overlook the interplay between sound and sight.

### E. Learning from acoustic feedback

Acoustic feedback can be used as an additional modality for robot control tasks. Liang *et al.* uses the acoustic vibration to estimate liquid height in a container in liquid pouring tasks [40]. Chen *et al.* propose an indoor audio-visual navigation task for localizing a sound source [41]. We consider a different problem setting and focus on voice-controlled robots that must understand sound commands correctly at the beginning of the robot’s task execution. We do not assume the availability of acoustic feedback during task execution and we consider all types of sounds, i.e., words, music tones, and environmental sounds, while [40], [41] consider only environmental sounds.

## III. METHODOLOGY

In this section, we describe our two-stage pipeline. In the first stage, we learn a representation for language grounding. In the second stage, we train a policy to learn skills.

### A. Representation learning from visual-audio data

The purpose of the first stage of our pipeline is to learn a joint representation of images and audios named VAR that associates the image of an object with its name in sound. To mimic the sensorimotor learning experiences of young children, the robot does not have access to the ground-truth labels of images and audios or the ground-truth pose information of the objects. The VAR environments act like children’s parents who tell the robot what it sees and does not see. For example, the environment acts like a mother saying, “This is an apple, not a banana,” when her child is looking at an apple.

To this end, we let the robot randomly move in the environment and automatically collect visual-audio triples  $(\mathbf{I}, \mathbf{S}^+, \mathbf{S}^-)$ , where  $\mathbf{I} \in \mathbb{R}^{n \times n}$  is the current RGB image from the robot’s camera,  $\mathbf{S}^+ \in \mathbb{R}^{l \times m}$  is the Mel Frequency Cepstral Coefficients (MFCC) [42] of the sound of object’s name, and  $\mathbf{S}^- \in \mathbb{R}^{l \times m}$  is the MFCC of the sound of some other object’s name. We use  $l$  to denote the number of frames in time axis and  $m$  to denote the number of features in frequency axis. The robot will hear nothing,  $\mathbf{S}^+ = \mathbf{0}_{l \times m}$ , if it does not trigger a sound. For the two tasks in Fig. 1, the empty sound happens when the TurtleBot does not see exactly one object or is too close to an object, and when the Kuka’s gripper tip is above none of the objects. During random exploration, the TurtleBot can observe the objects from various viewpoints, the Kuka can observe various spatial relations between the block and its gripper tip, and they can hear the same word said by different people.

Our goal is to encode both auditory and visual modalities into a joint latent space, where the embeddings of images and audios of the same object are close together, and those of different objects are far apart. We formulate the problem as metric learning and use triplet loss as the objective [43]. As shown in Fig. 2a, the VAR is a Siamese network that has three branches for encoding  $\mathbf{I}$ ,  $\mathbf{S}^+$ , and  $\mathbf{S}^-$ . We use  $f_S : \mathbb{R}^{l \times m} \rightarrow \mathbb{R}^d$  to encode both  $\mathbf{S}^+$  and  $\mathbf{S}^-$ , where  $d$  is the dimension of the latent space. We use  $f_I : \mathbb{R}^{n \times n} \rightarrow \mathbb{R}^d$  to encode  $\mathbf{I}$ . Both images and sounds are processed by a convolutional neural network (CNN). Rectangular filters are used in  $f_S$  since squared filters are not suitable for sound processing [44]. Then,  $\mathbf{v}^i = f_I(\mathbf{I})$ ,  $\mathbf{v}^+ = f_S(\mathbf{S}^+)$ , and  $\mathbf{v}^- = f_S(\mathbf{S}^-)$  are the latent representation of  $\mathbf{I}$ ,  $\mathbf{S}^+$ , and  $\mathbf{S}^-$ , respectively. We enforce the length of  $\mathbf{v}^i$ ,  $\mathbf{v}^+$ , and  $\mathbf{v}^-$  to be 1 by applying a  $L2$ -normalization, such that the latent space lives on a unit hypersphere as shown in Fig. 2b.

Triplet loss encourages the distance of vector embeddings between the anchor and the negative to be greater than that between the anchor and the positive by a margin of  $\alpha$ . We choose  $\mathbf{I}$  to be the anchor,  $\mathbf{S}^+$  to be the positive, and  $\mathbf{S}^-$  to be the negative. The objective for optimizing  $f_I$  and  $f_S$  with a visual-audio triple  $(\mathbf{I}, \mathbf{S}^+, \mathbf{S}^-)$  is

$$\mathcal{L}_{\text{VAR}} = \max(0, \|\mathbf{v}^i - \mathbf{v}^+\|_2^2 - \|\mathbf{v}^i - \mathbf{v}^-\|_2^2 + \alpha) \quad (1)$$

## B. RL with visual-audio representation

The second stage of our pipeline is to train the robot to reach goals using RL and the trained VAR. We model this interaction as a Markov Decision Process (MDP), defined by the tuple  $\langle \mathcal{X}, \mathcal{A}, P, R, \gamma \rangle$ . At each time step  $t$ , the agent receives a current observation  $x_t \in \mathcal{X}$  and takes an action  $a_t \in \mathcal{A}$  based on its policy  $\pi_\theta(a_t|x_t)$  parameterized by  $\theta$ . In return, the agent receives a reward  $r_t$  and transitions to the next state  $x_{t+1}$  according to an unknown state transition  $P(\cdot|x_t, a_t)$ . The process continues until  $t$  exceeds the maximum episode length  $T$  and the next episode starts. The goal of the agent is to maximize the expected return,  $R_t = \mathbb{E}[\sum_{i=t}^T \gamma^{i-t} r_i]$ , where  $\gamma$  is a discount factor. The value function  $V^\pi(x)$  is defined as the expected return starting from  $x$ , and successively following policy  $\pi$ .

At each time step  $t$ , the agent receives an image  $\mathbf{I}_t$  from its camera, the MFCC of the current sound  $\mathbf{S}_t$ , and robot states  $\mathbf{M}_t$  such as end-effector location or odometry. The current sound  $\mathbf{S}_t$  is triggered in the same way as  $\mathbf{S}^+$  in Sec. III-A. At  $t = 0$ , the agent receives an additional one-time sound command  $\mathbf{S}^g$  referring to an object in the scene. We define the state  $x_t \in \mathcal{X}$  for the MDP to be  $x_t = [\mathbf{I}_t, f_I(\mathbf{I}_t), f_S(\mathbf{S}^g), \mathbf{M}_t]$ , where  $f_I$  and  $f_S$  come from the VAR which is fixed in this stage of the pipeline. In addition to compactly representing the high-dimensional observations, the VAR also generates intrinsic reward function which motivates the agent to reach the target and replicate the sound command. Suppose the embeddings of an object in image and its name in sound are close to each other in VAR, the intrinsic reward function is

$$r_t = f_I(\mathbf{I}_t) \cdot f_S(\mathbf{S}^g) + f_S(\mathbf{S}_t) \cdot f_S(\mathbf{S}^g) \quad (2)$$

Intuitively, the agent receives high reward when both the object it sees and the current sound it hears match the sound command. Note that the current sound  $\mathbf{S}_t$  is not part of the state  $x_t$  and is only used to calculate the reward  $r_t$ . Thus, the robot policy is not conditioned on  $\mathbf{S}_t$  and does not require sound feedback at test time. Extrinsic reward functions rely on task-specific or robot-specific ground-truth information from the simulator, e.g., distance between the gripper tip and the target block for the Kuka environment. In contrast, our intrinsic reward function depends on the similarity of the embeddings and is thus agnostic to tasks and robots. Our policy network architecture is illustrated in Fig. 2c. The network takes  $x_t$  as input and output the value  $V(x_t)$  and the policy  $\pi(a_t|x_t)$ . We use Proximal Policy Optimization (PPO), a model-free policy gradient algorithm, for policy and value function learning [45]. We adopt the implementation from [46].

To successfully solve the more challenging TurtleBot environment, the method in [5] pretrains part of the network and uses auxiliary losses during optimization, which requires explicit ground-truth labels of sound and images and extra data collection. Our method achieves the same goal in a self-supervised manner. The portion of the network to be pretrained is in green in Fig. 2c, whose loss contains two

components. The first component  $\mathcal{L}_t$  is a binary classification loss that predicts whether the target object is in  $\mathbf{I}_t$ . The optimization of  $\mathcal{L}_t$  does not need extra data. Instead, the training data come directly from the visual-audio triples by splitting the triples to  $(\mathbf{I}, \mathbf{S}^+)$  with label 1 and  $(\mathbf{I}, \mathbf{S}^-)$  with label 0. In addition to  $\mathcal{L}_t$ , the second component uses knowledge distillation [47]. We treat  $f_V$  in Fig. 2c to be the student network and  $f_I$  in the VAR to be the teacher network. Let  $\mathcal{L}_d$  be the loss for the distillation. The total loss for the pretraining using an visual-audio triple is then

$$\mathcal{L}_{pre} = \mathcal{L}_d + \mathcal{L}_t, \quad \mathcal{L}_d = \|f_I(\mathbf{I}) - f_V(\mathbf{I})\|_2^2 \quad (3)$$

In RL training, we continue to finetune the network with only  $\mathcal{L}_t$  using the VAR. Specifically, we consider the label to be 1 if  $f_I(\mathbf{I}) \cdot f_S(\mathbf{S}^g) > 0.5$  and 0 otherwise.

Let the PPO loss be denoted as  $\mathcal{L}_{pg}$ . Our loss function for the policy network is

$$\mathcal{L}_p = \mathcal{L}_{pg} + w_t \mathcal{L}_t \quad (4)$$

where  $w_t$  is the scalar weight for  $\mathcal{L}_t$ . We set  $w_t = 1$  for the TurtleBot environment and  $w_t = 0$  for the Kuka environment. Our pipeline does not jointly optimize the representation and the RL agent, so the language grounding and skill learning are decoupled.

## IV. SIMULATION EXPERIMENTS

In this section, we first briefly describe the sound data processing and the two robotic environments for the simulated experiments. Then, we show the advantages of our pipeline over the method in [5] in both environments.

### A. Sound data processing

We consider various types of sounds including single-word speech signals, environmental sounds, single-tone signals, and a mixture of sounds among them. For speech signals, we choose “zero,” “one,” “two,” and “three” as Wordset1 and “house,” “tree,” “bird,” and “dog” as Wordset2 from the Speech Commands Dataset [48]. For environmental sounds, we use “car horn,” “gun shot,” “dog bark,” and “jackhammer” from UrbanSound8K Dataset [49]. For single-tone signals, we choose four musical notes,  $C_4$  (Middle C),  $D_4$ ,  $E_4$ , and  $F_4$ , performed by various musical instruments from NSynth datasets [50]. We use the Mix dataset to show that our model can map different types of sounds to one object or concept. In the Mix dataset, the “tree” and the “bird” are the same as Wordset2, but the “house” is mixed with “jackhammer” and “dog” is mixed with “dog bark.” For each sound in the Speech Commands, NSynth, and the Mix dataset, 1,000 samples are used for training and 50 samples are used for testing. For each sound in the UrbanSound8K Dataset, 400 samples are used for training and 50 samples are used for testing. When extracting the MFCCs for the sound signals, we keep the number of frames  $l$  to be 100 and number of features  $m$  to be 40 using the implementation from [51].



## B. Robotic Environments

We use two simulated environments implemented using PyBullet [52] to show that our model can be applied to different robotic platforms and tasks.

1) *TurtleBot*: The TurtleBot environment consists of a  $2\text{m} \times 2\text{m}$  arena and four fixed-sized 3D objects: a cube, a sphere, a cone, and a cylinder. Each object is associated with one or two sound commands. The goal of the robot is to navigate to the object corresponding to a sound command. When an episode begins, the robot and the four objects are placed randomly in the arena. Let  $v_d$  be the desired transitional velocity and  $\phi_d$  be the desired angle. The action  $a$  is  $[\delta_v, \delta_a]^\top$ , where  $\delta_v$  and  $\delta_a$  are the change of  $v_d$  and the change of  $\phi_d$ , respectively. We apply a simple proportional control on the desired angle. We update  $v_d$  and  $\phi_d$  by

$$v_d[t] = 0.05\delta_v + v_d[t-1], \quad \phi_d[t] = 0.15\delta_a + \phi_d[t-1] \quad (5)$$

The size of the RGB image  $\mathbf{I}_t$  is  $96 \times 96$ . The robot state vector  $\mathbf{M}_t$  is  $[v_d[t], \phi_d[t]]^\top$ . The time horizon  $T$  is 80. The agent in the TurtleBot environment needs to learn exploration skills to find the target object as quickly as possible.

2) *Kuka*: The Kuka environment consists of a table and four identical blocks. The blocks are placed in a line parallel to one side of the table in front of the robot with even spacing. The gripper tip can only move within a certain range of the xy-plane above the table top. Each block is associated with one or two sound commands. The goal of the robot is to move its gripper tip on the top of the block corresponding to a sound command. When an episode begins, the locations of the gripper tip and the blocks are initialized randomly. Let  $d_x$  and  $d_y$  be the desired gripper tip location in  $x$  axis and  $y$  axis, respectively. The action  $a$  is  $[\delta_x, \delta_y]^\top$ , where  $\delta_x$  and  $\delta_y$  are the change of  $d_x$  and  $d_y$ , respectively. We update  $d_x$  and  $d_y$  by

$$d_x[t] = 0.01\delta_x + d_x[t-1], \quad d_y[t] = 0.01\delta_y + d_y[t-1] \quad (6)$$

We use position control for controlling the joints of the robot. The size of the RGB image  $\mathbf{I}_t$  is  $96 \times 96$ . The robot state vector  $\mathbf{M}_t$  is  $[p_x[t], p_y[t]]^\top$ , where  $p_x[t]$  and  $p_y[t]$  are the gripper tip location at time  $t$ . The time horizon  $T$  is 100. The agent in the Kuka environment needs to develop spatial reasoning skills that can differentiate the target object from the four identical blocks using their relative positional information observed from only one location-fixed camera.

## C. Experiment setup

We now introduce the training and evaluation of our pipeline in simulation. We use our pipeline to solve both the TurtleBot and the Kuka environment with each of the five sets of sound commands. In our experiments, the overall settings are kept the same for solving both the TurtleBot and the Kuka environments, except that part of the TurtleBot’s policy network needs to be pretrained as shown in Sec. III-B and the network has more trainable parameters.

We first let the robot randomly explore the environment and collect 50,000 audio-visual triples. Using the triples, we

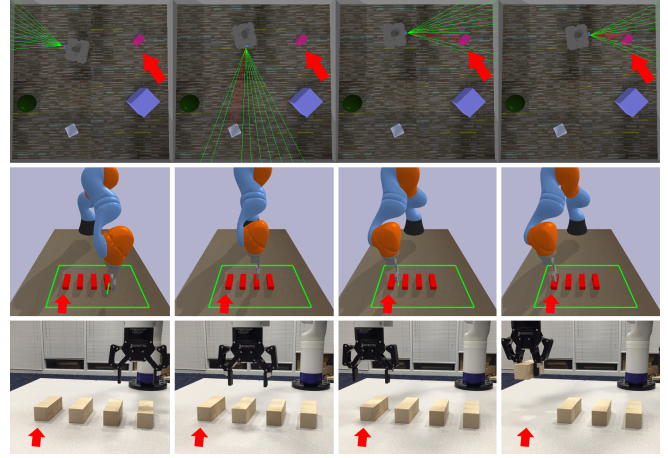


Fig. 3: **Qualitative Result in the simulation and the real world.** The target objects are indicated by the red arrows. Green and red lines are invisible to the robots. *Top*: Simulated TurtleBot searches and approaches its target, the purple cylinder. *Middle*: Kuka-IIWA correctly chooses the left most block in the simulator. *Bottom*: The real Kinova Gen3 moves its gripper to the target block and performs a successful grasp.

train a VAR for 30 epochs with learning rate  $1e^{-3}$ . The triplet margin  $\alpha \in [1.0, 1.2]$  and the latent space dimension  $d$  is 3. During RL training, the VAR is not updated and 8 instances of the environment run in parallel for collecting the agent’s experiences. The learning rate for the RL training is  $8e^{-6}$ .

1) *Evaluation criteria*: We test the trained policy for 50 episodes for each target object (200 episodes in total) with unheard sound data. For the Kuka environment, an episode is considered a success if the robot’s gripper stays close to the target block for more than 50 timesteps. For the TurtleBot environment, we define an episode as a success if the robot stays close to the target object for more than 5 timesteps. Our metric is success rate, defined as the percentage of successful episodes in all test episodes.

2) *Baselines*: We use the method in [5] as our baseline. The baseline method has access to extrinsic reward functions and ground-truth labels for the images and sounds for its end-to-end RL training.

## D. Results

The following subsections outline our quantitative and qualitative assessment of the VAR and the control policies.

1) *Quantitative comparison with the baseline*: We test the performance of our method and the baseline in both environments with different types of sounds. From the results in Table I, we find that our method generalizes well with respect to different types of sound commands and achieves high success rates on both the arm robot and mobile robot. Compared with the baseline, our method in general has 1%  $\sim$  5% improvements in success rates, even though it has no access to explicit ground-truth labels or extrinsic reward functions. We believe there are two reasons for this improvement: (1) Although the extrinsic reward functions in [5] are carefully hand-tuned, they may still be suboptimal and even be biased. In contrast, the intrinsic reward functions in our method come from robot’s own representations and thus require much less hand-tuning. (2) The method in [5]

TABLE I: Testing results of our method and the baseline method in both environments with different types of sounds.

Environment	Dataset	Success rate	
		[5]	Ours
TurtleBot	Wordset1	92.0	<b>94.0</b>
	Wordset2	89.5	<b>92.0</b>
	NSynth	95.0	<b>96.0</b>
	UrbanSound8K	<b>93.0</b>	<b>93.0</b>
	Mix	87.0	<b>91.0</b>
Kuka	Wordset1	95.5	<b>97.0</b>
	Wordset2	92.0	<b>95.0</b>
	NSynth	92.5	<b>98.0</b>
	UrbanSound8K	92.0	<b>94.0</b>
	Mix	94.0	<b>95.5</b>

jointly learns language grounding and control policies end-to-end via multiple losses, which may cause distractions to each other and thus the gradients on both tasks are biased. In contrast, our two-stage pipeline learns the two tasks separately, which benefits the training of both tasks. Fig. 3 shows the snapshots of the two robots successfully reaching their goals.

2) *Visualization of the VAR*: To better understand the VAR and how it produces an effective intrinsic reward for RL, we encode some positive pairs from the audio-visual triples with the trained VAR and plot the vector embeddings on a unit sphere, as shown in Fig. 4. We find that the embeddings of images and sounds of the same concept form a cluster and all clusters are separated from each other. Thus, the robots successfully associate images and sounds with the same meanings and distinguish those with different meanings, even though we do not explicitly classify the objects or inform the agent of the number of classes.

We also find that the VAR is able to map the images with ambiguous labels to meaningful locations on the spheres. For example, in Fig. 4a, the gripper tip in #2 is not directly above but is very close to Block 1, meaning that the label of #2 is something between Block 1 and Empty. In the VAR sphere, the vector embedding is indeed between the red and the cyan cluster. With the ability to represent ambiguous images, the VAR generates a relatively dense reward function that guides the robot exploration in RL. In the same example, suppose Block 1 is the target block, the dot products in Eq. 2 are higher in #2 than those in #4 or #5. Thus, the reward is higher when the gripper is around Block 1 and lower when the gripper is far away from Block 1. Similar observations can be found in TurtleBot in Fig. 4b, where #7 is between the cone and the empty cluster because the agent only see half of a cone.

## V. REAL-WORLD EXPERIMENTS

To show the application of our method on more robotic platforms and its effectiveness on real physical robots, we use a Kinova Gen3 arm for the Kuka choosing task, train the robot in the simulator, and deploy the trained model to a real Kinova Gen3 arm. We assign the four blocks from left to right with the words “zero,” “one,” “two,” and “three.”

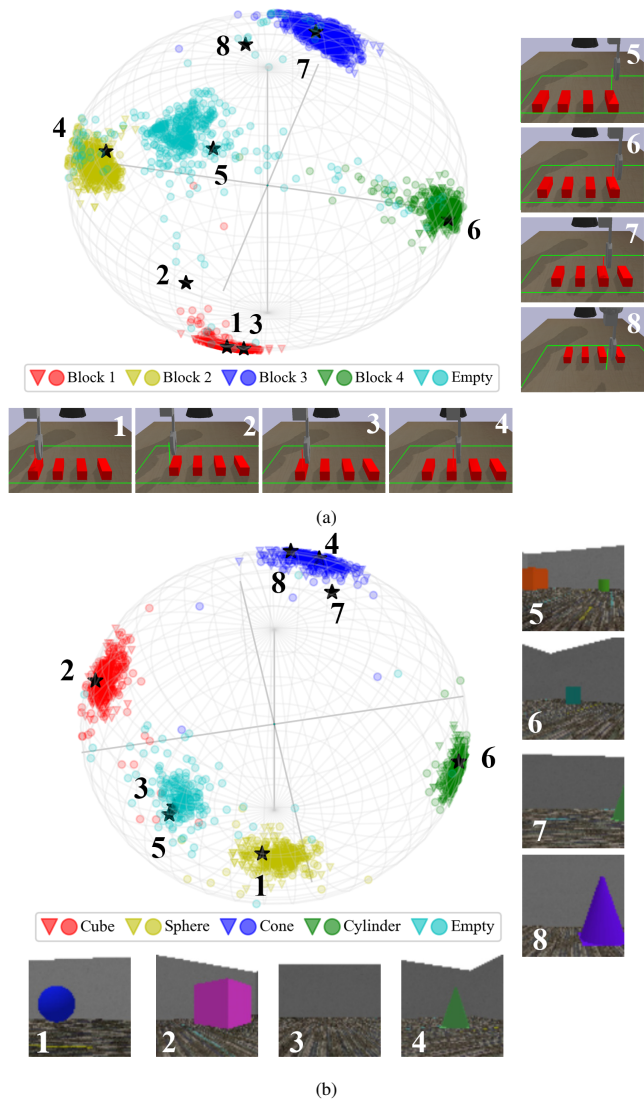


Fig. 4: **Visualizations of the VAR in both environments with Wordset1.** The colors indicate the ground truth labels of sound and image data. In the VAR spheres, the embeddings of images are marked by circles and sounds are marked by triangles. The black stars are the vector embeddings of the 8 images below each sphere. (a) Kuka environment: The block index increases from left to right. The “Empty” class consists of empty sounds and images of the gripper tip above none of the blocks. (b) TurtleBot environment: The “Empty” class consists of empty sounds and images with no object or more than one objects in view.

To narrow the gap between the simulated and the real world, we use domain randomization to learn robust features in both stages of our pipeline [53]. We randomize the color and texture of the blocks, table top, and the background using the textures from the Describable Textures Dataset during training [54]. We also randomize the the camera viewpoint and the relative positions among the blocks. Then, we deploy the model to a real Kinova Gen3 without further training on real-world data.

At every timestep, the trained agent receives an image from a location-fixed RGB camera and its end-effector location in the workspace. The wave files for testing from the sound datasets are used as the sound commands. The trained model controls the robot gripper to move towards the target block and adjusts its pre-grasp pose. At the end

of an episode, the robot lowers its two-finger parallel-jaw gripper vertically and perform a grasp on the chosen block.

We run a total of 40 tests (10 for each word) and count the number of times that the robot successfully grasps the block mentioned by the sound command. The results show that the success rate for “zero,” “one,” and “three” are all 90.0% and 100.0% for “two.” These results indicate that the simulation to real world transfer is successful in most cases. In the failure cases, the agent is able to move towards the correct block, but only fails at grasping because the block is not completely within its jaw. A typical successful episode is shown in Fig. 3.

## VI. CONCLUSION AND FUTURE WORK

Inspired by sensorimotor theory and children’s language acquisition, we propose a novel cognitive pipeline for vision-based voice-controlled robots. In our method, we first learn a visual-audio representation which associates images and sounds of the same concept. Then, we use the representation to generate an intrinsic reward function and embeddings for the downstream control tasks. Our method shows promising results and outperforms the end-to-end baseline with extrinsic reward functions across various types of sounds and robotic tasks in simulation. We also successfully transfer the policy trained in the simulator to a real robot. Possible directions to explore in the future work include: (1) generalizing the same visual-audio representation to different downstream tasks, (2) learning the representation in a self-supervised way without labeled triplets, and (3) using sound interpretation as a building block towards robot language acquisition and human-robot interaction.

## ACKNOWLEDGEMENTS

This work is supported by Agriculture and Food Research Initiative (AFRI) grant no. 2020-67021-32799/project accession no.1024178 from the USDA National Institute of Food and Agriculture. We thank Neeloy Chakraborty for feedback on paper drafts.

## REFERENCES

- [1] F. Stramandinoli, V. Tikhonoff, U. Pattacini, and F. Nori, “Grounding speech utterances in robotics affordances: An embodied statistical language model,” in *Joint IEEE International Conference on Development and Learning and Epigenetic Robotics (ICDL-EpiRob)*, 2016, pp. 79–86.
- [2] Y. Tada, Y. Hagiwara, H. Tanaka, and T. Taniguchi, “Robust understanding of robot-directed speech commands using sequence to sequence with noise injection,” *Frontiers in Robotics and AI*, vol. 6, p. 144, 2020.
- [3] K. M. Hermann, F. Hill, S. Green, F. Wang, R. Faulkner, H. Soyer, D. Szepesvari, W. M. Czarnecki, M. Jaderberg, D. Teplyashin, *et al.*, “Grounded language learning in a simulated 3d world,” *arXiv preprint arXiv:1706.06551*, 2017.
- [4] D. Serdyuk, Y. Wang, C. Fuegen, A. Kumar, B. Liu, and Y. Bengio, “Towards end-to-end spoken language understanding,” in *International Conference on Acoustics, Speech, and Signal Processing (ICASSP)*. IEEE, 2018, pp. 5754–5758.
- [5] P. Chang, S. Liu, H. Chen, and K. Driggs-Campbell, “Robot sound interpretation: Combining sight and sound in learning-based control,” in *IEEE/RSJ International Conference on Intelligent Robots and Systems (IROS)*. IEEE, 2020, pp. 5580–5587.
- [6] S. Harnad, “The symbol grounding problem,” *Physica D: Nonlinear Phenomena*, vol. 42, no. 1-3, pp. 335–346, 1990.
- [7] M. Alomari, P. Duckworth, D. Hogg, and A. Cohn, “Natural language acquisition and grounding for embodied robotic systems,” in *AAAI Conference on Artificial Intelligence (AAAI)*, vol. 31, no. 1, 2017.
- [8] J. K. O’Regan, *Why red doesn’t sound like a bell: Understanding the feel of consciousness*. Oxford University Press, 2011.
- [9] A. Clark, “Vision as dance? three challenges for sensorimotor contingency theory,” 2006.
- [10] L. Jacquey, G. Baldassarre, V. G. Santucci, and J. K. O’regan, “Sensorimotor contingencies as a key drive of development: from babies to robots,” *Frontiers in neurobotics*, vol. 13, p. 98, 2019.
- [11] H. H. Clark and S. E. Brennan, “Grounding in communication,” 1991.
- [12] Y. Bisk, A. Holtzman, J. Thomason, J. Andreas, Y. Bengio, J. Chai, M. Lapata, A. Lazaridou, J. May, A. Nisnevich, N. Pinto, and J. Turian, “Experience grounds language,” in *Conference on Empirical Methods in Natural Language Processing (EMNLP)*. Association for Computational Linguistics, 2020, pp. 8718–8735.
- [13] R. A. S. Fernandez, J. L. Sanchez-Lopez, C. Sampedro, H. Bavlé, M. Molina, and P. Campoy, “Natural user interfaces for human-drone multi-modal interaction,” in *IEEE International Conference on Unmanned Aircraft Systems (ICUAS)*, 2016, pp. 1013–1022.
- [14] E. Bastianelli, D. Croce, A. Vanzo, R. Basili, and D. Nardi, “A discriminative approach to grounded spoken language understanding in interactive robotics,” in *International Joint Conference on Artificial Intelligence (IJCAI)*, 2016, pp. 2747–2753.
- [15] R. Paul, J. Arkin, D. Aksaray, N. Roy, and T. M. Howard, “Efficient grounding of abstract spatial concepts for natural language interaction with robot platforms,” *The International Journal of Robotics Research*, vol. 37, no. 10, pp. 1269–1299, 2018.
- [16] A. Magassouba, K. Sugiura, A. T. Quoc, and H. Kawai, “Understanding natural language instructions for fetching daily objects using gan-based multimodal target–source classification,” *IEEE Robotics and Automation Letters*, vol. 4, no. 4, pp. 3884–3891, 2019.
- [17] B. Burger, I. Ferrané, F. Lerasle, and G. Infantes, “Two-handed gesture recognition and fusion with speech to command a robot,” *Autonomous Robots*, vol. 32, no. 2, pp. 129–147, 2012.
- [18] H. Chen, H. Tan, A. Kuntz, M. Bansal, and R. Alterovitz, “Enabling robots to understand incomplete natural language instructions using commonsense reasoning,” in *IEEE International Conference on Robotics and Automation (ICRA)*. IEEE, 2020, pp. 1963–1969.
- [19] R. Liu and X. Zhang, “A review of methodologies for natural-language-facilitated human–robot cooperation,” *International Journal of Advanced Robotic Systems*, vol. 16, no. 3, 2019.
- [20] A. Vanzo, D. Croce, E. Bastianelli, R. Basili, and D. Nardi, “Robust spoken language understanding for house service robots,” *Polibits*, no. 54, pp. 11–16, 2016.
- [21] J. Twiefel, T. Baumann, S. Heinrich, and S. Wermter, “Improving domain-independent cloud-based speech recognition with domain-dependent phonetic post-processing,” in *AAAI Conference on Artificial Intelligence (AAAI)*, 2014.
- [22] C. Fischer, M. Buss, and G. Schmidt, “Human-robot-interface for intelligent service robot assistance,” in *IEEE International Workshop on Robot and Human Communication*. IEEE, 1996, pp. 177–182.
- [23] J. Savage, D. A. Rosenblueth, M. Matamoros, M. Negrete, L. Contreras, J. Cruz, R. Martell, H. Estrada, and H. Okada, “Semantic reasoning in service robots using expert systems,” *Robotics and Autonomous Systems*, vol. 114, pp. 77–92, 2019.
- [24] *Speech model pre-training for end-to-end spoken language understanding*, 2019.
- [25] S. Bhosale, I. Sheikh, S. H. Dumpala, and S. K. Koppurapu, “End-to-end spoken language understanding: Bootstrapping in low resource scenarios,” in *Annual Conference of the International Speech Communication Association (INTERSPEECH)*, 2019, pp. 1188–1192.
- [26] M. Kim, G. Kim, S.-W. Lee, and J.-W. Ha, “St-bert: Cross-modal language model pre-training for end-to-end spoken language understanding,” in *International Conference on Acoustics, Speech, and Signal Processing (ICASSP)*. IEEE, 2021, pp. 7478–7482.
- [27] P. Wang, L. Wei, Y. Cao, J. Xie, and Z. Nie, “Large-scale unsupervised pre-training for end-to-end spoken language understanding,” in *International Conference on Acoustics, Speech, and Signal Processing (ICASSP)*. IEEE, 2020, pp. 7999–8003.
- [28] P. Anderson, Q. Wu, D. Teney, J. Bruce, M. Johnson, N. Sünderhauf, I. Reid, S. Gould, and A. van den Hengel, “Vision-and-language navigation: Interpreting visually-grounded navigation instructions in real environments,” in *IEEE Computer Society Conference on Computer Vision and Pattern Recognition (CVPR)*, 2018, pp. 3674–3683.

- [29] H. Chen, A. Suhr, D. Misra, N. Snaveley, and Y. Artzi, "Touchdown: Natural language navigation and spatial reasoning in visual street environments," in *IEEE Computer Society Conference on Computer Vision and Pattern Recognition (CVPR)*, 2019, pp. 12 538–12 547.
- [30] H. Yu, H. Zhang, and W. Xu, "Interactive grounded language acquisition and generalization in a 2d world," in *International Conference on Learning Representations (ICLR)*, 2018.
- [31] D. S. Chaplot, K. M. Sathyendra, R. K. Pasumarthi, D. Rajagopal, and R. Salakhutdinov, "Gated-attention architectures for task-oriented language grounding," in *Thirty-Second AAAI Conference on Artificial Intelligence (AAAI)*, 2018, pp. 2819–2826.
- [32] L. Smith and M. Gasser, "The development of embodied cognition: Six lessons from babies," *Artificial life*, vol. 11, no. 1-2, pp. 13–29, 2005.
- [33] M. Wellsby and P. M. Pexman, "Developing embodied cognition: Insights from children's concepts and language processing," *Frontiers in psychology*, vol. 5, p. 506, 2014.
- [34] S. Lange, M. Riedmiller, and A. Voigtländer, "Autonomous reinforcement learning on raw visual input data in a real world application," in *The international joint conference on neural networks (IJCNN)*. IEEE, 2012, pp. 1–8.
- [35] A. Nair, V. Pong, M. Dalal, S. Bahl, S. Lin, and S. Levine, "Visual reinforcement learning with imagined goals," in *Advances in Neural Information Processing Systems (NeurIPS)*, vol. 31, 2018.
- [36] Y. Wang, G. N. Narasimhan, X. Lin, B. Okorn, and D. Held, "Roll: Visual self-supervised reinforcement learning with object reasoning," in *Conference on Robot Learning (CoRL)*, 2020.
- [37] P. Sermanet, C. Lynch, Y. Chebotar, J. Hsu, E. Jang, S. Schaal, S. Levine, and G. Brain, "Time-contrastive networks: Self-supervised learning from video," in *IEEE International Conference on Robotics and Automation (ICRA)*. IEEE, 2018, pp. 1134–1141.
- [38] E. Jang, C. Devin, V. Vanhoucke, and S. Levine, "Grasp2vec: Learning object representations from self-supervised grasping," in *Conference on Robot Learning (CoRL)*, 2018.
- [39] T. Nguyen, N. Gopalan, R. Patel, M. Corsaro, E. Pavlick, and S. Tellex, "Robot Object Retrieval with Contextual Natural Language Queries," in *Proceedings of Robotics: Science and Systems*, 2020.
- [40] H. Liang, S. Li, X. Ma, N. Hendrich, T. Gerkmann, and J. Zhang, "Making sense of audio vibration for liquid height estimation in robotic pouring," in *IEEE/RSJ International Conference on Intelligent Robots and Systems (IROS)*, 2019.
- [41] C. Chen, U. Jain, C. Schissler, S. V. A. Gari, Z. Al-Halah, V. K. Ithapu, P. Robinson, and K. Grauman, "Soundspaces: Audio-visual navigation in 3d environments," in *European Conference on Computer Vision (ECCV)*. Springer, 2020, pp. 17–36.
- [42] S. Davis and P. Mermelstein, "Comparison of parametric representations for monosyllabic word recognition in continuously spoken sentences," *IEEE transactions on acoustics, speech, and signal processing*, vol. 28, no. 4, pp. 357–366, 1980.
- [43] F. Schroff, D. Kalenichenko, and J. Philbin, "Facenet: A unified embedding for face recognition and clustering," in *IEEE Computer Society Conference on Computer Vision and Pattern Recognition (CVPR)*, 2015, pp. 815–823.
- [44] D. Harwath, A. Torralba, and J. R. Glass, "Unsupervised learning of spoken language with visual context," in *Advances in Neural Information Processing Systems (NeurIPS)*, 2017.
- [45] J. Schulman, F. Wolski, P. Dhariwal, A. Radford, and O. Klimov, "Proximal policy optimization algorithms," *arXiv preprint arXiv:1707.06347*, 2017.
- [46] I. Kostrikov, "Pytorch implementations of reinforcement learning algorithms," <https://github.com/ikostrikov/pytorch-a2c-ppo-acktr-gail>, 2018.
- [47] C. Bucilua, R. Caruana, and A. Niculescu-Mizil, "Model compression," in *International conference on Knowledge discovery and data mining (SIGKDD)*, 2006, pp. 535–541.
- [48] P. Warden, "Speech commands: A dataset for limited-vocabulary speech recognition," *arXiv preprint arXiv:1804.03209*, 2018.
- [49] J. Salamon, C. Jacoby, and J. P. Bello, "A dataset and taxonomy for urban sound research," in *International Conference on Multimedia (ACM-MM)*, Orlando, FL, USA, Nov. 2014, pp. 1041–1044.
- [50] J. Engel, C. Resnick, A. Roberts, S. Dieleman, D. Eck, K. Simonyan, and M. Norouzi, "Neural audio synthesis of musical notes with wavenet autoencoders," in *International Conference on Machine Learning (ICML)*, 2017, pp. 1068–1077.
- [51] J. Lyons, "Python speech features," [https://github.com/jameslyons/python\\_speech\\_features](https://github.com/jameslyons/python_speech_features), 2013–2019.
- [52] E. Coumans and Y. Bai, "Pybullet, a python module for physics simulation for games, robotics and machine learning," <http://pybullet.org>, 2016–2019.
- [53] J. Tobin, R. Fong, A. Ray, J. Schneider, W. Zaremba, and P. Abbeel, "Domain randomization for transferring deep neural networks from simulation to the real world," *IEEE/RSJ International Conference on Intelligent Robots and Systems (IROS)*, pp. 23–30, 2017.
- [54] M. Cimpoi, S. Maji, I. Kokkinos, S. Mohamed, and A. Vedaldi, "Describing textures in the wild," in *IEEE Computer Society Conference on Computer Vision and Pattern Recognition (CVPR)*, 2014.